IAI Journals.ASM.org

Epicutaneous Model of Community-Acquired *Staphylococcus aureus* Skin Infections

Ranjani Prabhakara,[a] Oded Foreman,[b] Roberto De Pascalis,[a] Gloria M. Lee,[a] Roger D. Plaut,[a] Stanley Y. Kim,[a] Scott Stibitz,[a] Karen L. Elkins,[a] Tod J. Merkel[a]

Center for Biologics Evaluation and Research, FDA, Bethesda, Maryland, USA[a]; The Jackson Laboratory, Sacramento, California, USA[b]

Staphylococcus aureus **is one of the most common etiological agents of community-acquired skin and soft tissue infection (SSTI). Although the majority of *S. aureus* community-acquired SSTIs are uncomplicated and self-clearing in nature, some percentage of these cases progress into life-threatening invasive infections. Current animal models of *S. aureus* SSTI suffer from two drawbacks: these models are a better representation of hospital-acquired SSTI than community-acquired SSTI, and they involve methods that are difficult to replicate. For these reasons, we sought to develop a murine model of community-acquired methicillin-resistant *S. aureus* SSTI (CA-MRSA SSTI) that can be consistently reproduced with a high degree of precision. We utilized this model to begin to characterize the host immune response to this type of infection. We infected mice via epicutaneous challenge of the skin on the outer ear pinna using Morrow-Brown allergy test needles coated in *S. aureus* USA300. When mice were challenged in this model, they developed small, purulent, self-clearing lesions with predictable areas of inflammation that mimicked a human infection. CFU in the ear pinna peaked at day 7 before dropping by day 14. The T_h1 and T_h17 cytokines gamma interferon (IFN-γ), interleukin-12 (IL-12) p70, tumor necrosis factor alpha (TNF-α), IL-17A, IL-6, and IL-21 were all significantly increased in the draining lymph node of infected mice, and there was neutrophil recruitment to the infection site. *In vivo* neutrophil depletion demonstrated that neutrophils play a protective role in preventing bacterial dissemination and fatal invasive infection.**

Methicillin-resistant *Staphylococcus aureus* (MRSA) quickly gained notoriety after its emergence in the early 1960s (1) for its significant involvement in nosocomial infections, where it remains the most frequently isolated pathogen in hospital-acquired pneumonia and surgical site infection cases (2, 3). Recent trends indicate that *S. aureus* is no longer confined to the hospital setting and is increasingly responsible for community-associated (CA) infections in healthy individuals with no classic risk factors (3–5). CA-MRSA is now the most common etiologic agent of skin and soft tissue infection (SSTI) in patients admitted to emergency rooms and outpatient clinics in the United States, and 75% of all CA-MRSA infections present as SSTIs (6). In the United States, the prevalent strain type of *S. aureus* isolated from CA-MRSA infections is USA300, which accounts for 97% of *S. aureus* SSTIs (6).

S. aureus is capable of producing a wide variety of toxins, the expression of which differs between hospital-acquired MRSA (HA-MRSA) and CA-MRSA strains (7). Several staphylococcal toxins play pathogenic roles in staphylococcal SSTI, including Panton-Valentine leukocidin (PVL), which is associated with furuncles and skin abscesses, alpha-toxin, which is associated with dermonecrosis, and exfoliative toxins, which are associated with impetigo and scalded skin syndrome (8–10). USA300 has been shown to have enhanced virulence in animal models of infection (11) and express a large number of SSTI-associated toxins (12). There are also notable differences in disease presentation and progression. Unlike wound and surgical site infections, CA-MRSA SSTIs generally begin as small lesions with areas of inflammation and necrotic tissue that are often mistaken for spider bites (13, 14). Upon diagnosis, a large percentage of these small lesions are found to be the result of CA-MRSA SSTI (15, 16).

While the majority of CA-MRSA SSTIs in healthy individuals are effectively cleared by the host immune response, a small percentage of these cases progress to fatal invasive infections, even in patients with no known risk factors (17, 18). In mouse models, protective host responses involve recognition of *S. aureus* ligands by the innate immune system through Toll-like receptors and NOD-like receptors, which can lead to the production of the inflammatory cytokines interleukin-6 (IL-6) and IL-1 (19). Another key component of an effective host response against *S. aureus* SSTI is neutrophil recruitment and survival (20–22). Previous studies in mice have also demonstrated that the adaptive immune system can be involved in protection against *S. aureus* SSTI through epidermal production by T cells of IL-17 (23), a cytokine involved in neutrophil recruitment.

While these and other studies offer some insight into the factors involved in the establishment and progression of CA-MRSA SSTI, many aspects of bacterial virulence and the host immune response have yet to be elucidated. Novel animal model systems that mimic *S. aureus* SSTI would provide a useful tool not only for investigating such factors, but also for evaluating candidate vaccines for their potential to protect against *S. aureus* SSTI. Previous animal models of *Staphylococcus aureus* SSTI, however, largely mimic wound and surgical site infections, more representative of hospital-acquired infections, and have utilized methods of infection that are not easy to reproduce from animal to animal with

Received 28 November 2012 **Returned for modification** 24 December 2012
Accepted 27 January 2013
Published ahead of print 4 February 2013
Editor: J. B. Bliska
Address correspondence to Tod J. Merkel, tod.merkel@fda.hhs.gov.

doi:10.1128/IAI.01304-12

TABLE 1 Primers used in this work

Primer name	Sequence[a]	Use	Restriction site(s)
324	TAT GGTCTC CCCGGG ACCATGCTGAACAATTATTAGCTC	Δ*spa*	BsaI, XmaI
325	TAT GGTCTC ACGCGT AATGTTTTTCTTTTTCAAATTAATACCC	Δ*spa*	BsaI, MluI
326	TAT GGTCTC ACGCGT CGTCGTCGCGAACTATAAAAACAAACAATACAC	Δ*spa*	BsaI, MluI
354	TAT GGTCTC GGATCC TGTAGCAGCGAAACTTATTTCACC	Δ*spa*	BsaI, BamHI
408	ATA GCCGGC AATAGTTACCCTTATTATCAAGATAAG	*cat*	NgoMIV
480	TAT GGTCTC AGATCCCGAAAACCGACTGTAAAAAGTACAG	*cat*	BsaI
476	TAT GGTCTC AGATCCTTATGAGCTAGAAAGGCTTATGCAG	Δ*sbi*	BsaI
477	TAT GGTCTC TCGCGTCGAGATATATTTATTTTTCATGTGTATTCC	Δ*sbi*	BsaI
478	TAT GGTCTC TCGCGTAATTTATTATCATTCTGGAAATAATCAATC	Δ*sbi*	BsaI
479	TAT GGTCTC ATCGACTAAGCGTTTTCGAATTAACTGTTCG	Δ*sbi*	BsaI
528	TAT GGTCTC AGATCCTTTCTATGTAATGGCAAAATTTATTCCCGACG	HlaH35L	BsaI
533	TAT GGTCTC ATCGACTTCCAATTTGTTGAAGTCC	HlaH35L	BsaI
alphaUSIE	TAT GGTCTC GCATGCCATTTTCTTTATCATAAGTG	HlaH35L	BsaI
alphaDSIE	TAT GGTCTC ACATGCTCAAAAAAGTATTTTATAG	HlaH35L	BsaI

[a] Restriction sites are underlined.

precision. Many of these methods include disruption of the skin, such as by tape stripping (24), abrasion with a needle (25), or incision with a scalpel (26), followed by inoculation of the injured skin. Other methods include intradermal injection of *S. aureus* (23) or of dextran beads coated in *S. aureus* (27). We sought to develop a mouse model that mimics not a large wound or surgical site infection, but rather the smaller, superficial lesions often associated with CA-MRSA SSTIs. To this end, we developed a model in which the ear pinnae of mice were infected by pricking with *S. aureus*-coated Morrow-Brown allergy test needles (28). We characterized the progression of the disease through a variety of methods and examined host responses to *S. aureus* SSTI in our model. Here we show that epicutaneous infection using *S. aureus*-coated Morrow-Brown needles resulted in a consistently replicable, self-clearing SSTI that exhibited areas of neutrophil infiltration and inflammation, an increase in B cells, and higher levels of gamma interferon (IFN-γ), IL-12 p70, tumor necrosis factor alpha (TNF-α), IL-17A, IL-6, and IL-21 in the draining lymph node (LN). Importantly, survival of local infection was dependent on neutrophils.

CA-MRSA SSTI presents a very serious and costly health problem in the United States. Furthering our knowledge of how the host immune system clears this pathogen through the utilization of novel animal models of infection will help the scientific community to find better prophylactic and therapeutic strategies to battle these types of infections.

MATERIALS AND METHODS

Bacterial strains and preparation of needles. The clinical isolates of *S. aureus* used in these experiments were the USA300 strains NRS384 (NARSA), TCH1516 (ATCC) (29), and FPR3757 (ATCC) (30). The luminescent derivative of NRS384, SAP149, carries an integrated plasmid, pRP1190, which confers luminescence via a modified *luxBADCE* operon from *Photorhabdus luminescens* (31, 32) and confers chloramphenicol resistance via *cat*, originally from pC194 (33). In preliminary studies, we confirmed that there were no differences in infection outcome between USA300-lux and the parental USA300 strain (data not shown). The well-characterized USA300 strains TCH1516 and FPR3757 were used in these studies in order to ensure that infection results are consistent across different strains. In addition, two mutant strains of NRS384 were utilized to determine the effect of virulence defects in this model. The first mutant was a double-knockout strain deficient in two immunoglobulin binding proteins: staphylococcal protein A (SpA) and second binding protein of immunoglobulin (Sbi) (34). The second strain was a genetically inactivated mutant in the secreted toxin alpha-hemolysin (Hla). An overnight culture was started from *S. aureus* grown on tryptic soy agar (TSA) with 10 μg/ml chloramphenicol. A volume of 1.0 ml of the overnight culture was then diluted 1:50 in sterile tryptic soy broth with 10 μg/ml chloramphenicol, grown to an optical density at 600 nm (OD_{600}) of 0.8, washed in sterile phosphate-buffered saline (PBS), and resuspended at a concentration of 1.0×10^{11} CFU/ml. Ten microliters of *S. aureus* culture was dispensed onto the tip of a sterile Morrow-Brown allergy test needle using a sterile aerosol barrier pipette tip.

Construction of mutant strains. Primers used to engineer mutations in NRS384 are listed in Table 1. The backbone for all allelic exchange constructs was the shuttle vector pMAD (35). To genetically inactivate alpha-hemolysin, the chloramphenicol resistance gene *cat* (originally from pC194) (33) was amplified from pBT2 (36). The PCR product was digested with BsaI and inserted into BamHI-NgoMIV-digested pMAD, generating pRP1276. Using NRS384 as the template, DNA flanking the codon for histidine 35 of Hla was amplified by PCR. The two resulting PCR products were digested with BsaI and cloned (37) into pRP1276 that had been digested with BamHI and SalI, generating pRP1308, which carries the H35L mutation in the Hla sequence, previously shown to reduce hemolytic activity and virulence (38–41).

To delete *spa* from NRS384, flanking DNA was amplified, and the resulting PCR products were digested with BsaI and cloned into pMAD that had been digested with BamHI and SalI, generating pRP1161, which carries the modified *spa* sequence START + 17 codons + MluI site + 5 codons + STOP. To add the chloramphenicol resistance cassette, pRP1161 and pRP1276 were digested with BamHI and BsaI, and the 8-kb fragment from the former was ligated with the 3-kb fragment of the latter, creating pRP1282. A similar approach was undertaken for deletion of *sbi*, leading to the generation of pRP1284, which carries the modified sequence START + 6 codons + MluI site + 7 codons + STOP. Plasmids were transferred to *S. aureus* RN4220 (42) by transformation (43) and were subsequently transduced to NRS384 using phage phi80 (44). Allelic exchange was conducted as described previously (35). The HlaH35L strain was designated SAP345, and the Δ*spa*Δ*sbi* mutant strain was designated SAP315.

Mice. Female BALB/c mice (6 to 8 weeks old) were purchased from Taconic (Derwood, MD). Mice were maintained under microisolator conditions in the CBER animal facility (Bethesda, MD), in accordance with protocols reviewed and approved by the CBER Institutional Animal Care and Use Committee (IACUC).

Infection model. Six to eight mice per experimental group were epicutaneously challenged in the epidermis of the left ear. Mice were lightly anesthetized via intraperitoneal (i.p.) injection of 50 mg of ketamine/kg of

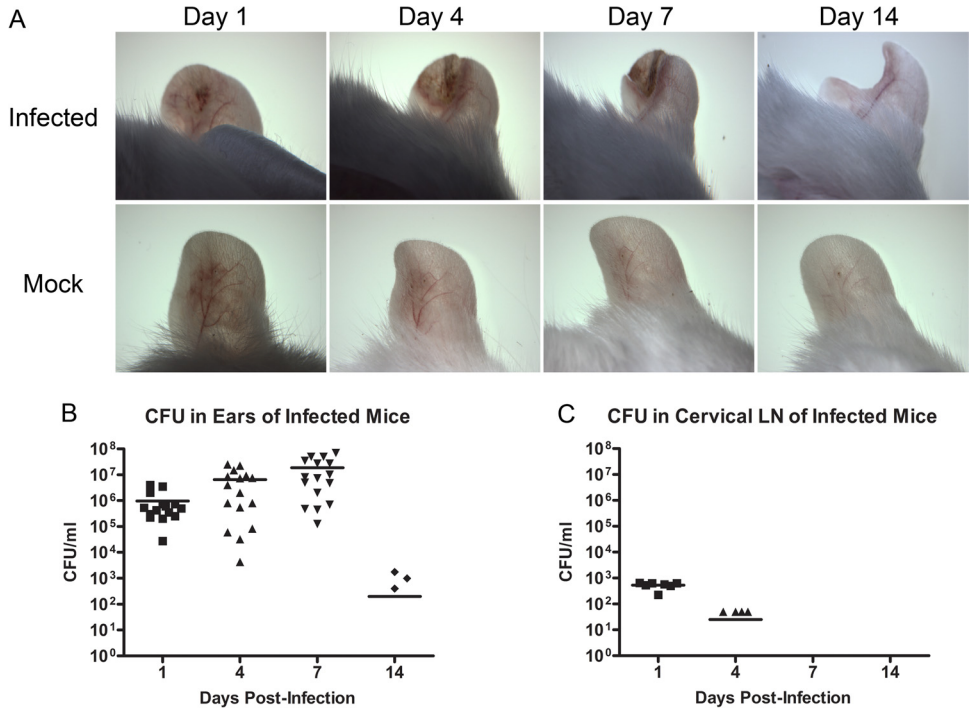

FIG 1 Development of acute localized SSTI after epicutaneous challenge of the ear pinna. (A) Dissecting microscope images of infected versus mock-infected pinnal skin at days 1, 4, 7, and 14 postinfection. Infection results in measurable purulent lesions demonstrating areas of inflammation and crusting. The same representative animals are shown for all four time points. Data points are visible only for animals with CFU. Serial dilutions of pinna (B) and cervical LN (C) homogenates were plated on TSA plates for CFU at days 1, 4, 7, and 14 postinfection ($n = 6$ to 8 mice per group; experiments performed in triplicate; limit of detection = 50 CFU/ml).

body weight (Ketaject; Phoenix Pharmaceuticals, Inc., St. Joseph, MO) and 5 mg xylazine/kg of body weight (AnaSed; LLOYD Laboratories, Inc., Shenandoah, IA). The left ear of each mouse was cleansed with 70% isopropanol before pricking the ear 10 times with an *S. aureus*-coated or sterile uncoated Morrow-Brown allergy test needle. The mean inoculating dose of *S. aureus* was determined to be 4.0×10^7 CFU/lesion, as determined by plating serial dilutions of ear pinna homogenates 4 h after inoculation (standard deviation [SD] = 2×10^7).

Ear, LN, and kidney cultures. At 1, 4, 7, and 14 days postinfection, mice were euthanized, the left ear and abdomen were gently cleansed with 70% isopropanol, and the ear pinnae and superficial cervical lymph nodes (LNs) were removed using sterile scissors. Ear pinnae or cervical LNs were placed into 500 μl of sterile PBS per ear or LN, in individual 2-ml Eppendorf tubes. Ears and LNs were homogenized using a Polytron PT 1200 handheld homogenizer (Kinematica, Bohemia, NY) and serial 10-fold dilutions of ear and LN homogenates were plated on tryptic soy agar plates to enumerate viable *S. aureus* per milliliter of homogenate. For experiments evaluating CFU in the kidney, kidneys were removed from each mouse using sterile scissors and placed into 5 ml of sterile PBS per pair of kidneys. Kidney tissue was then homogenized and 10-fold dilutions of homogenates were plated, as described above.

Microscopy. At days 1, 4, 7, and 14 postinfection, mice were lightly anesthetized via i.p. injection of 50 mg/kg ketamine (Ketaject; Phoenix Pharmaceuticals, Inc., St. Joseph, MO) and 5 mg/kg xylazine (AnaSed; LLOYD Laboratories, Inc., Shenandoah, IA). The left ear of each mouse was then examined using a SMZ-745T zoom stereo microscope (Nikon, Melville, NY) with a 15× objective and 0.67× click stop, and images were gathered using a Micropublisher 3.3 real-time viewing camera (Nikon, Melville, NY).

Histology. Ear pinnae from infected and mock-infected mice, as well as ear pinnae from infected mice treated with either RB6-8C5 or IgG2b isotype control monoclonal antibodies (see below), were removed at days 1, 4, 7, and 14 postinfection and fixed in formalin. Paraffin-embedded sections were stained with hematoxylin and eosin (H&E). All tissue processing and staining were performed by Histoserv, Inc. (Germantown, MD). Each ear section was examined under a Zeiss AX10 microscope (Thornwood, NY), and images were captured using a Zeiss AxioCam camera (Thornwood, NY). Slides were examined under blinded conditions on a scale of 1 to 5 by a board-certified veterinary pathologist, where 1 indicated minimal to mild focal dermal inflammatory infiltrates with or without dermal acanthosis, 2 indicated mild multifocal dermal infiltrates with or without intraepidermal microabscesses, 3 indicated multifocal to diffuse moderate dermal inflammatory infiltrates extending to the skeletal muscles with or without intraepidermal microabscesses, 4 indicated marked dermal inflammatory infiltrates extending to the skeletal muscle and cartilage with or without intraepidermal microabscesses, and 5 indicated full thickness auricular necrosis or massive inflammation with myositis and chondritis.

Cytokine production assay. Superficial cervical LNs were harvested from infected and uninfected mice at days 1, 4, and 7 postinfection. LNs were placed in 150 μl sterile Procarta cytokine standard diluent for cell lysate samples (Affymetrix, Santa Clara, CA) and homogenized on ice using a Polytron PT 1200 handheld homogenizer (Kinematica, Bohemia, NY) on the lowest speed setting. LN homogenates were centrifuged for 15 min at 14,000 × *g* at 4°C, and supernatants were stored at −70°C until ready to analyze. Samples were analyzed using Procarta Immunoassays (Santa Clara, CA) and read on a BioPlex 200 Luminex System (Bio-Rad, Hercules, CA) according to the manufacturer's directions. The cytokines tested included murine IFN-γ, IL-12 p70, TNF-α, IL-17A, IL-6, and IL-21.

Flow cytometry. Superficial cervical LNs were harvested from infected and mock-infected mice at days 4 and 7 postinfection, and single cell suspensions were prepared by homogenization using a Polytron PT 1200 handheld homogenizer (Kinematica, Bohemia, NY) followed by straining

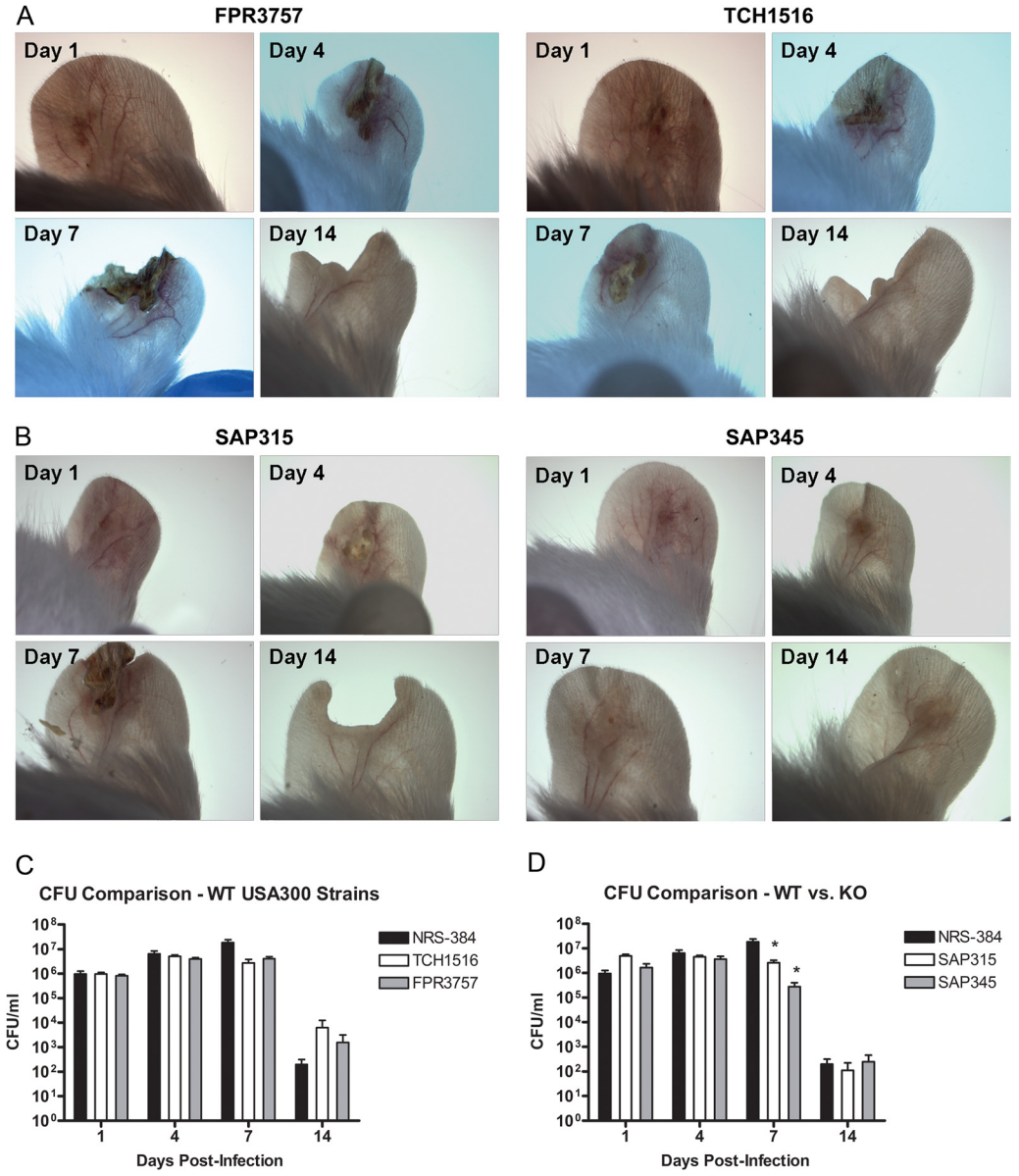

FIG 2 Comparison of pinnal skin after SSTI with wild-type or knockout (KO) USA300 strains. Dissecting microscope images at days 1, 4, 7, and 14 postinfection with TCH1516 or FPR3757 (A) and SpA/Sbi double knockout (SAP315) or Hla knockout (SAP345) (B) strains. Wild-type strains resulted in similar lesions to NRS384, while the Hla mutant strain resulted in decreased lesion severity. Serial dilutions of pinna homogenates from mice infected with wild-type (C) and mutant (D) strains were plated on TSA plates for CFU at days 1, 4, 7, and 14 postinfection ($n = 6$ to 8 mice per group; limit of detection = 50 CFU/ml; *, $P < 0.05$ compared to controls by Student's t test). Bars represent SD.

through a 0.40-μm cell strainer (BD Falcon, Franklin Lakes, NJ). Cell suspensions were then washed and resuspended in flow cytometry buffer (PBS-2% serum). Nonspecific binding of antibodies was inhibited by blocking Fc receptors with anti-CD16 (BD Pharmingen, San Jose, CA) for 10 min on ice. To discriminate live cells from dead cells, LN cells were stained using a commercially available live/dead staining kit (Invitrogen, Grand Island, NY) according to the manufacturer's directions. Cell suspensions were then washed in flow cytometry buffer and stained for cell surface markers using antibody concentrations that were previously optimized for use in seven- to nine-color staining protocols and isotype-matched control antibodies. The following antibodies were used: anti-CD45 (clone 30-F11), anti-B220 (clone RA3-6B2), anti-CD19 (clone 1D3), anti-TCRβ (clone H57-597), anti-CD4 (clone RM4-5), anti-CD8β (H35-17.2), anti-NK1.1 (clone PK136), anti-CD11b (clone M1/70), anti-Gr-1/Ly6G (clone RB6-8C5), and anti-CD11c (clone HL3), each labeled with a variety of fluorochromes (BD Pharmingen, San Jose, CA). All analyses were performed on live $CD45^+$ cells gated by comparison of forward scatter A versus forward scatter W. Cells were then analyzed for surface markers to quantify each cell type population.

***In vivo* neutrophil depletion.** To determine if neutrophils play a role in bacterial clearance during *S. aureus* SSTI, BALB/c mice were injected i.p. with 500 μg of the neutrophil-depleting monoclonal antibody RB6-8C5 (BioXCell, West Lebanon, NH) to neutralize neutrophils *in vivo*. RB6-8C5 can also potentially deplete inflammatory monocytes. Control mice received i.p. injections of rat IgG2 isotype control monoclonal antibody (BioXCell, West Lebanon, NH). Monoclonal antibodies were injected 24 h before *S. aureus* SSTI. Mice received subsequent i.p. injections of 500 μg every 72 h postinfection to maintain reduced neutrophil levels

for the duration of the experiment. Neutrophil depletion throughout the course of the experiment was analyzed by flow cytometry using heparinized blood stained with anti-Gr-1 (clone RB6-8C5). Mice were euthanized at days 1, 4, 7, and 14 postimplantation. Ear pinnae, cervical LNs, and kidneys were harvested and processed, and serial dilutions of tissue homogenates were plated on tryptic soy agar plates to enumerate CFU/ml, as described above. Microscope and *in vivo* imaging system (IVIS) images were also captured, as described below. Mice were also observed daily for mortality throughout the duration of the experiment.

***In vivo* imaging of cervical LNs.** The progression of *S. aureus* SSTI was followed by acquiring whole body images of neutrophil-depleted mice using an IVIS100 *in vivo* imaging system (Caliper Life Sciences, Hopkinton, MA). Mice were anesthetized with 2.5% isoflurane mixed with oxygen delivered by the gas anesthesia system supplied with the IVIS100. Ventral images were acquired to determine the presence of bioluminescent *S. aureus* in the cervical LN. All images were acquired using an exposure time of 3 min, according to the manufacturer's recommendations. Images were analyzed using Living Image 4.1 software (Caliper Life Sciences, Hopkinton, MA).

Statistical analysis. CFU levels were compared between mice infected with the USA300 strains NRS384, TCH1516, or FPR3757 and between mice infected with NRS384, a Sbi/Spa mutant strain, or an Hla mutant strain. CFU levels were also compared between infected mice that had been treated with either RB6-8C5 or an isotype control antibody. Lesion severity was compared between infected and mock-infected ear sections and between infected RB6-8C5 and isotype control-treated mice. In addition, cytokine levels and immune cell percentages in the draining lymph node were compared between infected and mock-infected control mice. All analyses were performed using GraphPad Prism. Differences in CFU levels, lesion severity, cytokine levels, and immune cell percentages were evaluated using a two-tailed Student's *t* test, with a *P* value of <0.05 indicating statistical significance.

RESULTS

Epicutaneous infection using an *S. aureus*-coated Morrow-Brown needle results in replicable, self-limiting skin infection. Ear pinnae from BALB/c mice were infected via epicutaneous challenge with *S. aureus*. Each mouse was then examined under a dissecting microscope at days 1, 4, 7, and 14 postinfection to determine lesion development and severity. Results indicated the consistent development of replicable purulent lesions at the infection site with clear and predictable areas of inflammation and epidermal crusting, which were not present in mock-infected control mice. An increase in the size and severity of lesions was observed between days 1 and 7 postinfection, followed by resolution of the infection by day 14 (Fig. 1A). CFU were enumerated from homogenized ear tissue to determine the bacterial load in the ear at each time point postinfection. Results demonstrated that viable *S. aureus* was cultured out of the pinnae of the ear at days 1, 4, and 7 postinfection, with a dramatic decrease in bacterial load that corresponded with the healing of lesions by day 14 (Fig. 1B). In addition, low numbers of *S. aureus* were observed in the cervical LNs at days 1 and 4 postinfection, but bacteria were no longer cultured from cervical LNs by day 7 postinfection (Fig. 1C). In order to demonstrate that the infection elicited by our *S. aureus* SSTI model was not unique to the NRS384 strain of USA300, we also infected BALB/c mice with two well-characterized wild-type (WT) USA300 strains: TCH1516, a strain derived from an otherwise healthy pediatric patient who developed severe sepsis (29), and FPR3757, a strain isolated from an abscess in an HIV-positive adult male (30). These strains were both able to produce SSTI in BALB/c mice with similar lesions and bacterial concentrations at the infection site comparable to that of NRS384 (Fig. 1A and 2A and C). In order to demonstrate that this infection model can be used to effectively identify virulence defects during *S. aureus* SSTI, we also infected BALB/c mice with two mutant strains, a SpA/Sbi double knockout and an Hla genetically inactivated mutant. These mutant strains both exhibited a reduction in bacterial load at day 7 postinfection compared to wild-type NRS384. In addition, infection with the Hla mutant resulted in significantly decreased lesion severity compared to infection with the wild type (Fig. 1A and 2B and D).

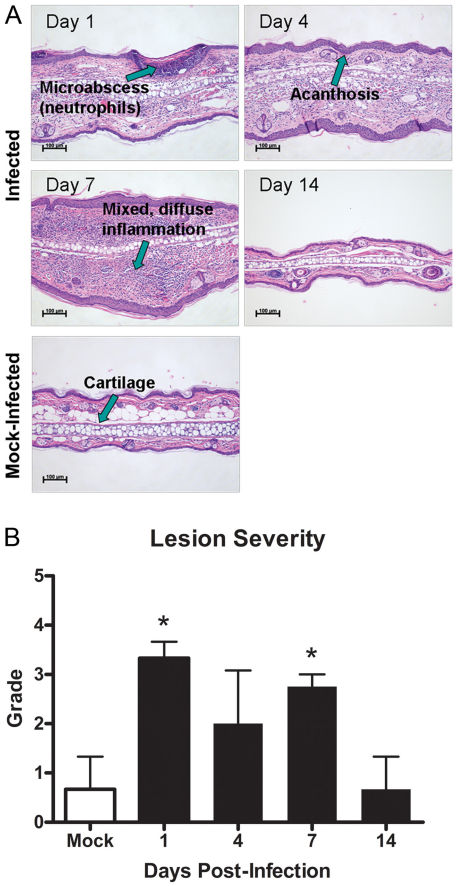

FIG 3 Histopathology of *S. aureus* SSTI lesions. Ear pinnae were harvested from infected and mock-infected BALB/c mice, and paraffin-embedded sections were stained with hematoxylin and eosin before examination under a light microscope. (A) Neutrophil infiltration, inflammation, and acanthosis are evident at the infection site for infected but not mock-infected mice. (B) Lesions are more severe on a scale of 1 to 5 in infected versus mock-infected mice ($n = 3$ to 4 mice per group; experiments performed in duplicate; *, $P < 0.05$ compared to controls by Student's *t* test). Bars represent SD.

Lesion pathology resulting from *S. aureus* epicutaneous infection. In order to evaluate pathology at the lesion site during this skin infection, paraffin-embedded ear pinna sections from infected BALB/c mice were compared to ear sections from mock-infected BALB/c mice. Mock-infected control ear sections did not show significant pathology. However, infected ear pinnae had moderate to severe lesions as early as day 1 postinfection, as demonstrated by the presence of deep dermal abscesses, multifocal intradermal microabscesses, and neutrophilic dermatitis (Fig. 3A). By day 4 postinfection, ear pinnae began to show diffuse dermal infiltrates comprised of neutrophils and macrophages, areas of acanthosis, and epidermal crusting. By day 7 postinfection, lesions

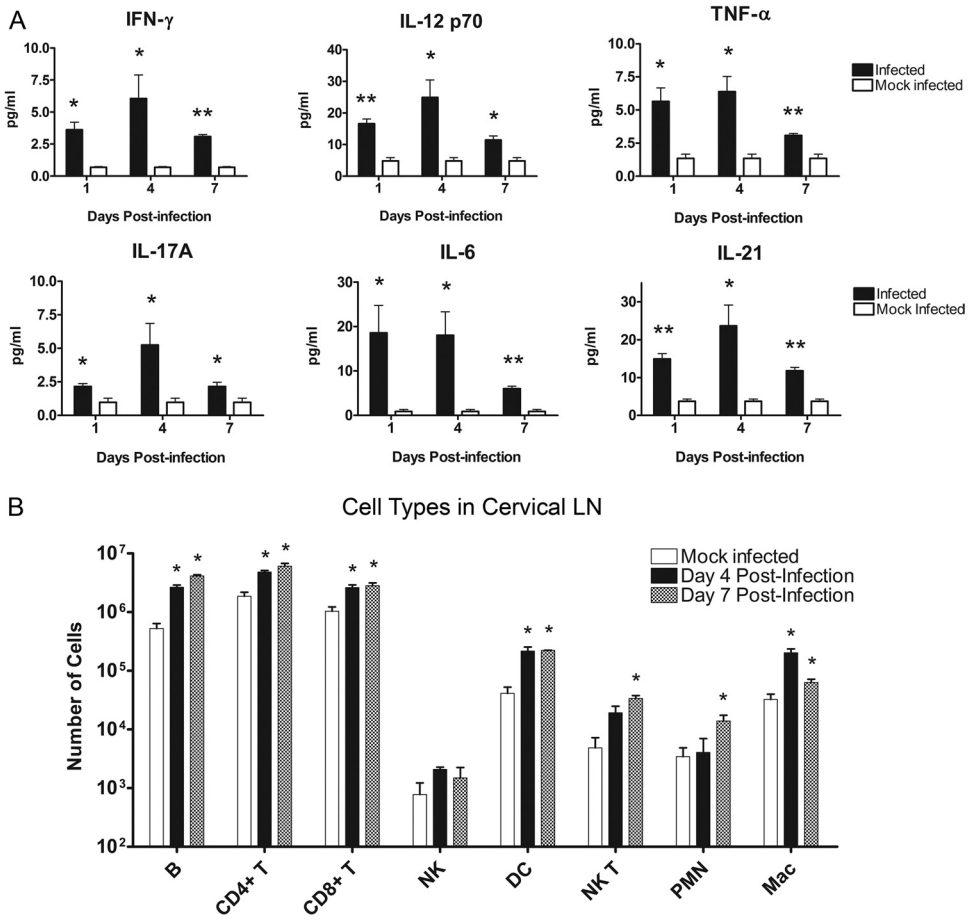

FIG 4 Cytokine and immune cell profiles in the draining LN. Cervical LNs were removed from BALB/c mice after epicutaneous challenge with *S. aureus*-coated or mock infection with uncoated Morrow-Brown needles. (A) Supernatants from LN homogenates were analyzed for cytokines at days 1, 4, and 7 postinfection ($n = 6$ to 9 mice per group; experiments performed in duplicate; *, $P < 0.05$ compared to controls by Student's *t* test; **, $P < 0.01$ compared to controls by Student's *t* test). Bars represent SD. (B) Single-cell suspensions of LN cells at days 4 and 7 postinfection were prepared, and cell surface markers were stained with fluorescent antibodies. Samples were analyzed via flow cytometry ($n = 3$ mice per group; experiments performed in triplicate; *, $P < 0.05$ compared to controls by Student's *t* test). Bars represent SD.

uniformly exhibited deep multifocal mixed dermal infiltrates, myositis, and areas of acanthosis. By day 14 postinfection, ear pinna skin began to return to normal and no longer exhibited any significant lesions, although there was generally permanent loss of ear tissue at the infection site (Fig. 3A). Lesion severity, as measured on a scale from 1 to 5, was significantly higher in infected mice at days 1 and 7 postinfection, versus mock-infected mice, but returned to similar levels by day 14 (Fig. 3B).

***S. aureus* SSTI results in increased T_h1, T_h2, and T_h17 cytokines in BALB/c mice.** Cytokine levels in the draining LNs were compared between infected and mock-infected BALB/c mice in order to determine the character of the immune response. At days 1, 4, and 7 postinfection, cervical LNs were removed from infected and mock-infected mice and homogenized. LN homogenates were then analyzed using a Luminex-based cytokine assay. Several T_h1 associated cytokines were elevated in the draining LNs throughout the course of infection, including IFN-γ, IL-12 p70, and TNF-α. There were also significantly higher levels of the T_h17-associated cytokines IL-6, IL-17, and IL-21 in infected animals relative to mock-infected controls (Fig. 4A). Cytokine levels generally peaked at day 4 postinfection and began to drop off by day 7, with the exception of IL-6, which peaked at day 1. These cytokines remained significantly elevated over mock-infected controls at all time points tested. A number of chemokines involved with neutrophil recruitment were also elevated in the cervical LN, including KC, MIP-1α, and CXCL5. In contrast, the T_h2 and regulatory T cell (T_{reg})-associated cytokine, IL-10, was unchanged between infected and mock-infected controls (data not shown).

***S. aureus* SSTI results in elevation of several immune cell populations in the draining LNs of BALB/c mice.** Numbers of various immune cell types were determined via flow cytometry analyses in order to further elucidate the character of the immune response to *S. aureus* SSTI. At day 4 and day 7 postinfection, cervical LNs were removed from infected and mock-infected mice, and single cell suspensions of LN cells were prepared and stained for various immune cell markers before being analyzed by flow cytometry. Results demonstrate significantly higher numbers of several immune cell types in the draining LNs of infected mice than control mice, including B cells, $CD4^+$ T cells, $CD8^+$ T cells, dendritic cells (DCs), natural killer T (NKT) cells, polymorphonuclear cells (PMNs), and macrophages (Fig. 4B). This increase was evident at both time points tested, with the exception of NKT

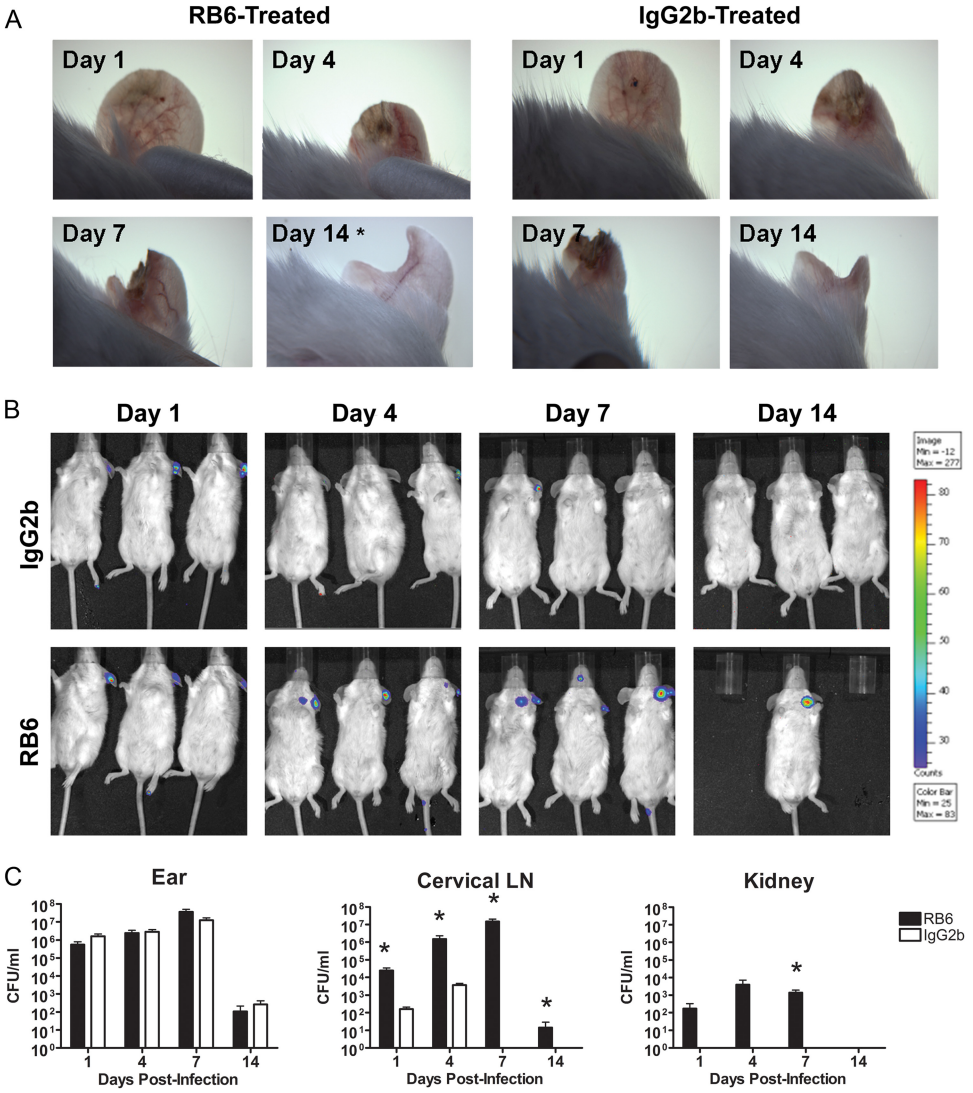

FIG 5 *S. aureus* SSTI progression in BALB/c mice after *in vivo* depletion of neutrophils. Dissecting microscope images of ear pinnae (A) and IVIS images of bioluminescent *S. aureus* in the cervical LNs (B) of RB6-8C5- versus IgG2b control-treated mice at days 1, 4, 7, and 14 postinfection. The same representative animals are shown for all four time points, with the exception of day 14 microscope image ($n = 9$ mice per group; experiments performed in triplicate; *, representative mouse surviving to day 14). (C) Serial dilutions of ear pinna, cervical LN, and kidney homogenates were plated on TSA plates at days 1, 4, 7, and 14 postinfection. CFU/ml were calculated and plotted over time ($n = 6$ to 8 mice per group; experiments performed in duplicate; limit of detection = 50 CFU/ml; *, $P < 0.05$ compared to IgG2b controls by Student's *t* test).

cells and PMNs, which were significantly higher only at day 7 postinfection.

Neutrophils are required to control dissemination of *S. aureus* during SSTI. The observation of infiltration of neutrophils into the localized site of infection and draining LNs suggested that these cells may play an important role in containment and clearance of infection. In order to test this, BALB/c mice were treated with either RB6-8C5 to deplete neutrophils *in vivo* or an IgG2b isotype control 24 h before epicutaneous infection with a bioluminescent strain of USA300. Following infection, mice were treated with either RB6-8C5 or the IgG2b isotype control every 72 h for the duration of the experiment. Each mouse was examined under a dissecting microscope and via whole-animal *in vivo* imaging on days 1, 4, 7, and 14 postinfection. In addition, ear pinnae, cervical LNs, and kidneys from neutrophil-depleted or isotype control-treated mice were harvested at the same time points, homogenized and plated for CFU, or fixed in formalin for H&E staining of paraffin-embedded sections. CFU in ear tissue homogenates were enumerated to determine the course of infection, and CFU in superficial cervical LN and kidney homogenates were enumerated to determine whether *S. aureus* disseminated out of the ear pinna. Microscope images (Fig. 5A) and CFU counts (Fig. 5C) indicate that there is no observable difference in the size, severity, or bacterial load of skin lesions on the ears of RB6-8C5- versus IgG2b-treated mice. In contrast, both IVIS images (Fig. 5B) and CFU counts (Fig. 5C) indicated increased bacterial burden over time in the cervical LNs of RB6-8C5-treated mice. In addition, *S. aureus* was cultured from the kidneys of only mice treated with RB6-8C5, a hallmark of bacterial dissemination (45) into the bloodstream (Fig. 5C). Histopathological analysis of infected ear

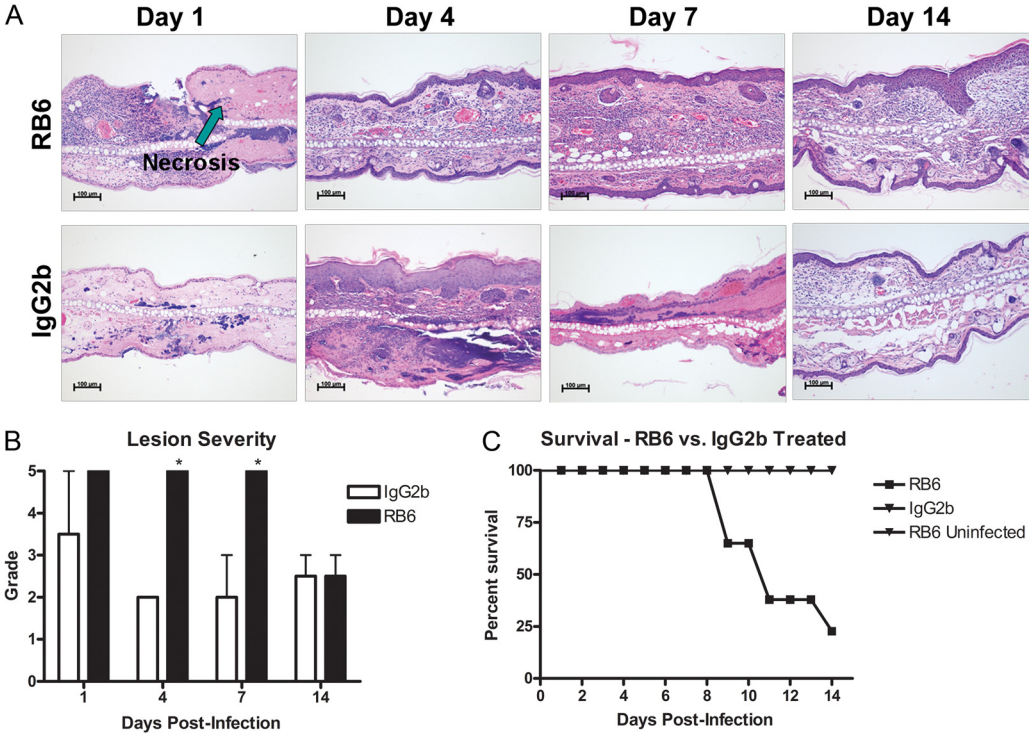

FIG 6 Histopathology of *S. aureus* SSTI lesions in RB6-8C5-treated or IgG2b-treated control mice. Ear pinnae were harvested from infected BALB/c mice that were treated with either RB6-8C5 to deplete neutrophils *in vivo* or an IgG2b isotype control. (A) Paraffin-embedded sections were stained with hematoxylin and eosin before examination under a light microscope. In contrast to control mice, neutrophil infiltration and abscess formation are not observed in neutrophil-depleted mice, but areas of necrosis are. (B) A lesion score of 1 to 5 was assigned by a blinded board-certified veterinary pathologist ($n = 2$ to 3 mice per group; performed in a single experiment; *, $P < 0.05$ compared to IgG2b controls by Student's t test). Bars represent SD. (C) Survival following *S. aureus* SSTI in RB6-8C5-treated versus isotype control mice ($n = 6$ to 8 mice per group; experiments performed in duplicate).

sections from RB6-8C5-treated versus control mice demonstrated that neutrophil depletion leads to extensive areas of necrosis not observed in nonneutropenic-infected mice (Fig. 6A), as well as increased severity of lesions, as measured on a scale of 1 to 5 (Fig. 6B).

Finally, mice were observed daily for survival. Results demonstrated that 80% of infected mice treated with RB6-8C5 died between days 8 and 14 after infection (Fig. 6C). This increase in mortality was observed only in RB6-treated mice subject to *S. aureus* SSTI. No mortality was observed in mock-infected, RB6-treated mice, confirming that death was due to the infection in the treated mice, not due to the administration of RB6-8C5. Depletion of neutrophils by treatment with RB6-8C5 monoclonal antibody was confirmed throughout these experiments by flow cytometry (data not shown).

DISCUSSION

S. aureus SSTI is an increasingly costly and common occurrence in healthy individuals outside the hospital environment (3–5). Although many of these infections are self-clearing, a small number of them progress to potentially fatal invasive infections (17, 18). CA-MRSA SSTIs generally differ from hospital-acquired SSTIs in how the infection initially manifests itself, as well as in the most prevalent disease-causing strains (6). However, established animal models of *S. aureus* SSTI are more representative of HA-MRSA infections, such as surgical site and wound infections. Other models of SSTI utilize methods that may be difficult to replicate with uniformity (24–26). In the present study, we sought to develop a murine model that accurately and consistently mimics CA-MRSA SSTI in humans and to characterize the host response against this type of infection using this model.

Morrow-Brown needles are designed for the performance of allergy skin prick testing in which consistent penetration of the epidermis is desired. The needles are specifically designed to ensure consistent depth of epidermal penetration and lesion size. Inoculation of the mouse epidermis of the ear pinnae using Morrow-Brown allergy test needles coated with *S. aureus* resulted in a consistently replicable purulent lesion that was small, localized, and self-clearing in immunocompetent BALB/c mice, an indication that this is a clinically relevant model of CA-MRSA SSTI that accurately mimics similar lesions in patients (13). In addition, the ease with which lesions of similar size, severity, and bacterial burden were achieved when using this model indicates that it will be a useful tool for studying these types of infections.

Lesions were characterized by areas of inflammation, purulence, and crusting (Fig. 1A), as well as neutrophil infiltration, abscess formation, and other signs of tissue inflammation and damage, such as myositis and acanthosis (Fig. 3A). Bacterial burdens and lesion severity increased between days 1 and 7 postinfection and subsequently dropped by day 14 (Fig. 1B and 3B), by which time lesions were resolved. A similar progression of infection was demonstrated when mice were infected with either of two additional strains of USA300, indicating that this infection model is consistent across multiple strains of *S. aureus* (Fig. 2A and C). In

contrast, infection with a SpA/Sbi double knockout or an Hla mutant strain of NRS384 resulted in low bacterial loads at the infection site at day 7 postinfection and, in the case of the Hla mutant, decreased lesion severity (Fig. 2B and D). These results indicate that this model also provides an effective method for identifying and studying bacterial factors that are potentially required for *S. aureus* pathogenesis. It is likely that the majority of *S. aureus* skin infections in humans resolve quickly and go unreported. Because the number of uncomplicated *S. aureus* infections is unknown, the rate at which these infections progress to serious infections requiring medical treatment cannot be calculated; nonetheless, it is reasonable to assume that the rate is very low in healthy individuals. This is consistent with our results indicating that the epicutaneous skin infection model accurately reflects *S. aureus* skin infections in humans.

In mouse models, it is known that a number of T_h1 and T_h17 cytokines are associated with protection against fatal *S. aureus* infection (46–48). This is especially true for the T_h17 response, which is associated with neutrophil recruitment and protection against extracellular bacteria (49–52). In the epicutaneous skin infection model, levels of the T_h1 cytokines IFN-γ, IL-12, and TNF-α and the T_h17 cytokines IL-17A, IL-6, and IL-21 in the draining cervical LNs were significantly elevated over controls at all time points tested and generally peaked at day 4 postinfection. The one exception was IL-6, which peaked at day 1, remained elevated at day 4, and then decreased at day 7 postinfection (Fig. 4A). In addition, there was an increase in the frequency of CD4 T cells, CD8 T cells, DCs, NKT cells, PMNs, and macrophages (Fig. 4B). This is not surprising, due to the large number of bacterial products produced by *S. aureus* that are known to activate various arms of the immune system (52). Based on these observations, we suspect that T_h1 and T_h17 responses enable the host to contain and resolve *S. aureus* skin infections; this idea may be tested in future studies.

Neutrophils were previously shown to play an essential role in the containment and clearance of *S. aureus* infections (52–54). Because neutrophils were clearly present at the infection site (Fig. 3A) and in the cervical LNs (Fig. 4B) of infected mice in this study, and there was a concomitant increase in T_h17 cytokines in the draining LNs (Fig. 4A), we examined the role of neutrophils in the epicutaneous skin infection model. Our results demonstrated that neutrophils play a critical role in the containment of *S. aureus* skin infections in this model. Although neutrophil depletion did not appear to affect lesion size (Fig. 5A) or bacterial burden at the site of infection (Fig. 5C), the severity of lesions was significantly higher in neutrophil-depleted mice (Fig. 5B), and neutrophil-depleted mice failed to contain the infection (Fig. 5C). In untreated mice, bacterial burdens were high at the site of infection, and small numbers of bacteria were observed in the draining LNs, but the infection did not spread beyond the draining LN; bacteria were ultimately cleared from the site of infection, and the lesions were resolved (Fig. 1C). In contrast, neutrophil-depleted mice were unable to contain the infection. Large numbers of bacteria were observed in the LNs of these mice, leading ultimately to disseminated disease and death (Fig. 5C and 6C). Our results therefore suggest that neutropenia is likely a risk factor for severe *S. aureus* skin and soft tissue infections. It should be noted that RB6-8C6 can also deplete inflammatory monocytes in the host. These cells may also play a protective role in this model, and further investigation is needed to determine if both of these cell types play a role in protection from *S. aureus* SSTI.

Taken together, results from these studies indicate that our model accurately mimics human infection while simultaneously providing a tool that allows for the consistent replication of experimental CA-MRSA SSTIs with ease and precision. This model results in SSTI lesions that share many similarities with CA-MRSA infections in patients (13, 15, 16), including the host's dependence upon neutrophils for the effective containment and clearance of the infection. Because CA-MRSA is an increasingly costly and dangerous public health threat in the United States, it is important to have the necessary tools to evaluate candidate vaccines, new antimicrobials, and other potentially therapeutic agents. This model may provide such a needed tool, and future studies will focus on further elucidating mechanisms of protection in the host and evaluating biomarkers of *S. aureus* SSTI.

ACKNOWLEDGMENTS

We thank Vanessa Kelly and Brandon Feinen for technical assistance with the animal models. We also thank Drusilla L. Burns, Rebecca A. Brady, and Christopher P. Mocca for their advice and assistance throughout this study.

Strain NRS384 was obtained through the Network on Antimicrobial Resistance in *Staphylococcus aureus* (NARSA), supported under NIAID, NIH contract no. N01-AI-95359.

REFERENCES

1. **Gordon RJ, Lowy FD.** 2008. Pathogenesis of methicillin-resistant *Staphylococcus aureus* infection. Clin. Infect. Dis. **46**(Suppl 5):S350–S359.
2. **Otto M.** 2010. Basis of virulence in community-associated methicillin-resistant *Staphylococcus aureus*. Annu. Rev. Microbiol. **64**:143–162.
3. **Lowy FD.** 1998. *Staphylococcus aureus* infections. N. Engl. J. Med. **339**: 520–532.
4. **Klevens RM, Morrison MA, Nadle J, Petit S, Gershman K, Ray S, Harrison LH, Lynfield R, Dumyati G, Townes JM, Craig AS, Zell ER, Fosheim GE, McDougal LK, Carey RB, Fridkin SK.** 2007. Invasive methicillin-resistant *Staphylococcus aureus* infections in the United States. JAMA **298**:1763–1771.
5. **Herold BC, Immergluck LC, Maranan MC, Lauderdale DS, Gaskin RE, Boyle-Vavra S, Leitch CD, Daum RS.** 1998. Community-acquired methicillin-resistant *Staphylococcus aureus* in children with no identified predisposing risk. JAMA **279**:593–598.
6. **Moran GJ, Krishnadasan A, Gorwitz RJ, Fosheim GE, McDougal LK, Carey RB, Talan DA.** 2006. Methicillin-resistant *S. aureus* infections among patients in the emergency department. N. Engl. J. Med. **355**:666–674.
7. **Naimi TS, LeDell KH, Como-Sabetti K, Borchardt SM, Boxrud DJ, Etienne J, Johnson SK, Vandenesch F, Fridkin S, O'Boyle C, Danila RN, Lynfield R.** 2003. Comparison of community- and health care-associated methicillin-resistant *Staphylococcus aureus* infection. JAMA **290**:2976–2984.
8. **Durupt F, Mayor L, Bes M, Reverdy ME, Vandenesch F, Thomas L, Etienne J.** 2007. Prevalence of *Staphylococcus aureus* toxins and nasal carriage in furuncles and impetigo. Br. J. Dermatol. **157**:1161–1167.
9. **Tkaczyk C, Hua L, Varkey R, Shi Y, Dettinger L, Woods R, Barnes A, MacGill RS, Wilson S, Chowdhury P, Stover CK, Sellman BR.** 2012. Identification of anti-alpha toxin monoclonal antibodies that reduce the severity of *Staphylococcus aureus* dermonecrosis and exhibit a correlation between affinity and potency. Clin. Vaccine Immunol. **19**:377–385.
10. **Mesrati I, Saidani M, Ennigrou S, Zouari B, Ben RS.** 2010. Clinical isolates of Pantone-Valentine leucocidin- and gamma-haemolysin-producing *Staphylococcus aureus*: prevalence and association with clinical infections. J. Hosp. Infect. **75**:265–268.
11. **Li M, Cheung GY, Hu J, Wang D, Joo HS, Deleo FR, Otto M.** 2010. Comparative analysis of virulence and toxin expression of global community-associated methicillin-resistant *Staphylococcus aureus* strains. J. Infect. Dis. **202**:1866–1876.
12. **Kobayashi SD, Malachowa N, Whitney AR, Braughton KR, Gardner**

DJ, Long D, Bubeck WJ, Schneewind O, Otto M, Deleo FR. 2011. Comparative analysis of USA300 virulence determinants in a rabbit model of skin and soft tissue infection. J. Infect. Dis. **204**:937–941.
13. **Cohen PR.** 2007. Community-acquired methicillin-resistant Staphylococcus aureus skin infections: implications for patients and practitioners. Am. J. Clin. Dermatol. **8**:259–270.
14. **Gorwitz RJ.** 2008. A review of community-associated methicillin-resistant Staphylococcus aureus skin and soft tissue infections. Pediatr. Infect. Dis.J. **27**:1–7.
15. **Suchard JR.** 2011. "Spider bite" lesions are usually diagnosed as skin and soft-tissue infections. J. Emerg. Med. **41**:473–481.
16. **Vozdecky C.** 2009. Community-acquired methicillin-resistant *Staphylococcus aureus*: not just a spider bite. Fam. Community Health **32**:76–84.
17. **Francis JS, Doherty MC, Lopatin U, Johnston CP, Sinha G, Ross T, Cai M, Hansel NN, Perl T, Ticehurst JR, Carroll K, Thomas DL, Nuermberger E, Bartlett JG.** 2005. Severe community-onset pneumonia in healthy adults caused by methicillin-resistant *Staphylococcus aureus* carrying the Panton-Valentine leukocidin genes. Clin. Infect. Dis. **40**:100–107.
18. **Zetola N, Francis JS, Nuermberger EL, Bishai WR.** 2005. Community-acquired meticillin-resistant *Staphylococcus aureus*: an emerging threat. Lancet Infect. Dis. **5**:275–286.
19. **Hruz P, Zinkernagel AS, Jenikova G, Botwin GJ, Hugot JP, Karin M, Nizet V, Eckmann L.** 2009. NOD2 contributes to cutaneous defense against *Staphylococcus aureus* through alpha-toxin-dependent innate immune activation. Proc. Natl. Acad. Sci. U. S. A. **106**:12873–12878.
20. **Molne L, Verdrengh M, Tarkowski A.** 2000. Role of neutrophil leukocytes in cutaneous infection caused by *Staphylococcus aureus*. Infect. Immun. **68**:6162–6167.
21. **Kim MH, Granick JL, Kwok C, Walker NJ, Borjesson DL, Curry FR, Miller LS, Simon SI.** 2011. Neutrophil survival and c-kit(+)-progenitor proliferation in *Staphylococcus aureus*-infected skin wounds promote resolution. Blood **117**:3343–3352.
22. **Rigby KM, Deleo FR.** 2012. Neutrophils in innate host defense against Staphylococcus aureus infections. Semin. Immunopathol. **34**:237–259.
23. **Cho JS, Pietras EM, Garcia NC, Ramos RI, Farzam DM, Monroe HR, Magorien JE, Blauvelt A, Kolls JK, Cheung AL, Cheng G, Modlin RL, Miller LS.** 2010. IL-17 is essential for host defense against cutaneous *Staphylococcus aureus* infection in mice. J. Clin. Invest. **120**:1762–1773.
24. **Onunkwo CC, Hahn BL, Sohnle PG.** 2010. Clearance of experimental cutaneous *Staphylococcus aureus* infections in mice. Arch. Dermatol. Res. **302**:375–382.
25. **Dai T, Tegos GP, Zhiyentayev T, Mylonakis E, Hamblin MR.** 2010. Photodynamic therapy for methicillin-resistant *Staphylococcus aureus* infection in a mouse skin abrasion model. Lasers Surg. Med. **42**:38–44.
26. **Cho JS, Zussman J, Donegan NP, Ramos RI, Garcia NC, Uslan DZ, Iwakura Y, Simon SI, Cheung AL, Modlin RL, Kim J, Miller LS.** 2011. Noninvasive in vivo imaging to evaluate immune responses and antimicrobial therapy against *Staphylococcus aureus* and USA300 MRSA skin infections. J. Investig. Dermatol. **131**:907–915.
27. **Bunce C, Wheeler L, Reed G, Musser J, Barg N.** 1992. Murine model of cutaneous infection with gram-positive cocci. Infect. Immun. **60**:2636–2640.
28. **Demoly P, Bousquet J, Manderscheid JC, Dreborg S, Dhivert H, Michel FB.** 1991. Precision of skin prick and puncture tests with nine methods. J. Allergy Clin. Immunol. **88**:758–762.
29. **Highlander SK, Hulten KG, Qin X, Jiang H, Yerrapragada S, Mason EO, Jr, Shang Y, Williams TM, Fortunov RM, Liu Y, Igboeli O, Petrosino J, Tirumalai M, Uzman A, Fox GE, Cardenas AM, Muzny DM, Hemphill L, Ding Y, Dugan S, Blyth PR, Buhay CJ, Dinh HH, Hawes AC, Holder M, Kovar CL, Lee SL, Liu W, Nazareth LV, Wang Q, Zhou J, Kaplan SL, Weinstock GM.** 2007. Subtle genetic changes enhance virulence of methicillin resistant and sensitive *Staphylococcus aureus*. BMC Microbiol. **7**:99.
30. **Diep BA, Gill SR, Chang RF, Phan TH, Chen JH, Davidson MG, Lin F, Lin J, Carleton HA, Mongodin EF, Sensabaugh GF, Perdreau-Remington F.** 2006. Complete genome sequence of USA300, an epidemic clone of community-acquired meticillin-resistant *Staphylococcus aureus*. Lancet **367**:731–739.
31. **Loving CL, Khurana T, Osorio M, Lee GM, Kelly VK, Stibitz S, Merkel TJ.** 2009. Role of anthrax toxins in dissemination, disease progression, and induction of protective adaptive immunity in the mouse aerosol challenge model. Infect. Immun. **77**:255–265.
32. **Meighen EA.** 1991. Molecular biology of bacterial bioluminescence. Microbiol. Rev. **55**:123–142.
33. **Horinouchi S, Weisblum B.** 1982. Nucleotide sequence and functional map of pC194, a plasmid that specifies inducible chloramphenicol resistance. J. Bacteriol. **150**:815–825.
34. **Atkins KL, Burman JD, Chamberlain ES, Cooper JE, Poutrel B, Bagby S, Jenkins AT, Feil EJ, van den Elsen JM.** 2008. *S. aureus* IgG-binding proteins SpA and Sbi: host specificity and mechanisms of immune complex formation. Mol. Immunol. **45**:1600–1611.
35. **Arnaud M, Chastanet A, Debarbouille M.** 2004. New vector for efficient allelic replacement in naturally nontransformable, low-GC-content, gram-positive bacteria. Appl. Environ. Microbiol. **70**:6887–6891.
36. **Bruckner R.** 1997. Gene replacement in *Staphylococcus carnosus* and *Staphylococcus xylosus*. FEMS Microbiol. Lett. **151**:1–8.
37. **Stemmer WP, Morris SK.** 1992. Enzymatic inverse PCR: a restriction site independent, single-fragment method for high-efficiency, site-directed mutagenesis. Biotechniques **13**:214–220.
38. **Bubeck WJ, Patel RJ, Schneewind O.** 2007. Surface proteins and exotoxins are required for the pathogenesis of *Staphylococcus aureus* pneumonia. Infect. Immun. **75**:1040–1044.
39. **Kennedy AD, Bubeck WJ, Gardner DJ, Long D, Whitney AR, Braughton KR, Schneewind O, Deleo FR.** 2010. Targeting of alpha-hemolysin by active or passive immunization decreases severity of USA300 skin infection in a mouse model. J. Infect. Dis. **202**:1050–1058.
40. **Menzies BE, Kernodle DS.** 1994. Site-directed mutagenesis of the alpha-toxin gene of *Staphylococcus aureus*: role of histidines in toxin activity in vitro and in a murine model. Infect. Immun. **62**:1843–1847.
41. **Rauch S, DeDent AC, Kim HK, Bubeck WJ, Missiakas DM, Schneewind O.** 2012. Abscess formation and alpha-hemolysin induced toxicity in a mouse model of *Staphylococcus aureus* peritoneal infection. Infect. Immun. **80**:3721–3732.
42. **Kreiswirth BN, Lofdahl S, Betley MJ, O'Reilly M, Schlievert PM, Bergdoll MS, Novick RP.** 1983. The toxic shock syndrome exotoxin structural gene is not detectably transmitted by a prophage. Nature **305**:709–712.
43. **Bae T, Glass EM, Schneewind O, Missiakas D.** 2008. Generating a collection of insertion mutations in the *Staphylococcus aureus* genome using bursa aurealis. Methods Mol. Biol. **416**:103–116.
44. **McNamara P.** 2012. Genetic manipulation of *Staphylococcus aureus*, p 89–129. *In* J. A. Lindsay (ed), *Staphylococcus*: molecular genetics. Caister Academic Press, Norfolk, United Kingdom.
45. **Doi K, Leelahavanichkul A, Yuen PS, Star RA.** 2009. Animal models of sepsis and sepsis-induced kidney injury. J. Clin. Invest. **119**:2868–2878.
46. **Watkins RL, Pallister KB, Voyich JM.** 2011. The SaeR/S gene regulatory system induces a pro-inflammatory cytokine response during *Staphylococcus aureus* infection. PLoS One **6**:e19939. doi:10.1371/journal.pone.0019939.
47. **Nakane A, Okamoto M, Asano M, Kohanawa M, Minagawa T.** 1995. Endogenous gamma interferon, tumor necrosis factor, and interleukin-6 in *Staphylococcus aureus* infection in mice. Infect. Immun. **63**:1165–1172.
48. **Joshi A, Pancari G, Cope L, Bowman E, Cua D, Proctor R, McNeely T.** 2012. Immunization with *Staphylococcus aureus* iron regulated surface determinant B (IsdB) confers protection via Th17/IL17 pathway in a murine sepsis model. Hum. Vaccin. Immunother. **8**:336–346.
49. **Wei L, Laurence A, O'Shea JJ.** 2008. New insights into the roles of Stat5a/b and Stat3 in T cell development and differentiation. Semin. Cell Dev. Biol. **19**:394–400.
50. **Siciliano NA, Skinner JA, Yuk MH.** 2006. *Bordetella bronchiseptica* modulates macrophage phenotype leading to the inhibition of CD4+ T cell proliferation and the initiation of a Th17 immune response. J. Immunol. **177**:7131–7138.
51. **Mizuno T, Ando T, Nobata K, Tsuzuki T, Maeda O, Watanabe O, Minami M, Ina K, Kusugami K, Peek RM, Goto H.** 2005. Interleukin-17 levels in *Helicobacter pylori*-infected gastric mucosa and pathologic sequelae of colonization. World J. Gastroenterol. **11**:6305–6311.
52. **Deleo FR, Diep BA, Otto M.** 2009. Host defense and pathogenesis in *Staphylococcus aureus* infections. Infect. Dis. Clin. North Am. **23**:17–34.
53. **Mayer-Scholl A, Averhoff P, Zychlinsky A.** 2004. How do neutrophils and pathogens interact? Curr. Opin. Microbiol. **7**:62–66.
54. **Roos D, van Bruggen R, Meischl C.** 2003. Oxidative killing of microbes by neutrophils. Microbes Infect. **5**:1307–1315.